



Universiteit
Leiden
The Netherlands

Stereochemical optimization of N,2-substituted cycloalkylamines as norepinephrine reuptake inhibitors

Dilweg, M.A.; Mocking, T.A.M.; Maragkoudakis, P.; Westen, G.J.P. van; Heitman, L.H.; IJzerman, A.P.; ... ; Es, D. van der

Citation

Dilweg, M. A., Mocking, T. A. M., Maragkoudakis, P., Westen, G. J. P. van, Heitman, L. H., IJzerman, A. P., ... Es, D. van der. (2024). Stereochemical optimization of N,2-substituted cycloalkylamines as norepinephrine reuptake inhibitors. *Rsc Medicinal Chemistry*, 15(12), 4068-4079. doi:10.1039/d4md00521j

Version: Publisher's Version

License: [Licensed under Article 25fa Copyright Act/Law \(Amendment Taverne\)](#)

Downloaded from: <https://hdl.handle.net/1887/4196785>

Note: To cite this publication please use the final published version (if applicable).

RESEARCH ARTICLE



Cite this: *RSC Med. Chem.*, 2024, 15, 4068

Stereochemical optimization of *N*,2-substituted cycloalkylamines as norepinephrine reuptake inhibitors†

Majlen A. Dilweg,^{‡a} Tamara A. M. Mocking,^{‡a} Pantelis Maragkoudakis,^a Gerard J. P. van Westen,^{‡a} Laura H. Heitman,^{ab} Adriaan P. IJzerman,^a Willem Jespers^{‡a} and Daan van der Es^{‡a*}

The norepinephrine transporter (NET), encoded by the SLC6A2 gene, is one of three key monoamine neurotransmitter transporters. Inhibition of NET-mediated reuptake of norepinephrine by monoamine reuptake inhibitors has been the main therapeutic strategy to treat disorders such as depression, ADHD and Parkinson's disease. Nevertheless, lack of efficacy as well as risk of adverse effects are still common for these treatments underscoring the necessity to improve drug discovery efforts for this target. In this study, we developed new inhibitors based on 4-((2-(3,4-dichlorophenyl)cyclopentyl)amino)butan-1-ol (**8**), a potent NET inhibitor, which emerged from earlier virtual screening efforts using a predictive proteochemometric model. Hence, we optimized the *N*,2-substituted cycloalkylamine scaffold in three regions to design twenty new derivatives. To establish structure–activity relationships for these NET inhibitors, all novel compounds were tested utilizing an impedance-based ‘transporter activity through receptor activation’ assay. Moreover, all stereoisomers of the most potent compound (**27**) were synthesized and evaluated for their inhibitory potencies. Initial screening indicated that modifications in the cyclopentylamine moiety and phenyl substitutions decreased NET inhibition compared to **8**, emphasizing the importance of the five-membered ring, secondary amine and dichloro-substitution pattern in NET binding. Substituting the original butylalcohol at the *R*² position with a rigid cyclohexanol yielded lead compound **27**, with potency similar to reference inhibitor nisoxetine. Pharmacological characterization of all eight stereoisomers of **27** revealed varying inhibitory potencies, favoring a *trans*-orientation of the *N*,2-substituted cyclopentyl moiety. Molecular docking highlighted key interactions and the impact of a hydrophilic region in the binding pocket. This study presents a novel set of moderate to highly potent NET inhibitors, elucidating the influence of molecular orientation in the NET binding pocket and offering valuable insights into drug discovery efforts for monoamine transport-related treatments.

Received 8th July 2024,
Accepted 11th September 2024

DOI: 10.1039/d4md00521j

rsc.li/medchem

Introduction

Several neurodegenerative and neuropsychiatric conditions such as Parkinson's disease, schizophrenia and depression are directly correlated to a dysregulation of monoamine neurotransmitter signaling in pre- and post-synaptic neurons.^{1–3} Consequently, manipulating the concentration and therefore signaling events of the monoamines

norepinephrine (NE), dopamine (DA) and serotonin (5-HT) in the synaptic cleft is a well-known therapeutic strategy in these types of disorders.^{4–6} Under standard physiological conditions, these neurotransmitters are released *via* synaptic vesicles from the presynaptic neuron into the synaptic cleft. Herein, reuptake of these neurotransmitters is predominantly facilitated by the monoamine transporters (MATs), which are integral plasma membrane proteins of the solute carrier superfamily.⁷ One of these MATs is the norepinephrine transporter (NET, SLC6A2), which is primarily expressed on the presynaptic terminals of noradrenergic neurons where it transports its endogenous substrates NE and DA in a Na⁺- and Cl[−]-dependent manner.^{8,9} As a consequence of the involvement in neurotransmission, inhibition of NET is clinically utilized to treat mood- and behavior-related indications. Hence, NET inhibitors are known as antidepressants, among other applications.

^a Division of Medicinal Chemistry, Leiden Academic Centre for Drug Research, Leiden University, Einsteinweg 55, 2333 CC Leiden, The Netherlands.

E-mail: d.van.der.es@lacdr.leidenuniv.nl

^b Oncode Institute, 2333 CC Leiden, The Netherlands

† Electronic supplementary information (ESI) available: Supplementary figures and experimental, ¹H NMR, ¹³C NMR, 2D NMR spectra and HPLC traces of the in-house synthesized compounds. See DOI: <https://doi.org/10.1039/d4md00521j>

‡ These authors contributed equally.

Atomoxetine (**1a**), reboxetine (**1b**, a racemic mixture of the (*S,S*)-(+)- and (*R,R*)-(–)-enantiomer) and maprotiline (**2**) are examples of marketed reuptake inhibitors that selectively target NET, *e.g.*, selective norepinephrine reuptake inhibitors (NRIs, Fig. 1), which are used in the treatment of attention deficit hyperactivity disorder (ADHD)¹⁰ and major depression disorder (MDD).¹¹ However, these drugs exhibit multiple drawbacks, including slow onset of action¹² and partial therapeutic efficacy.¹³ To address these issues, multiple dual-acting agents (norepinephrine–dopamine reuptake inhibitors (NDRIs) and serotonin–norepinephrine reuptake inhibitors (SNRIs)) were developed leading to improved safety profiles and patient tolerability compared to NRIs.¹⁴ This resulted in clinically approved drugs such as dexamethylphenidate (**4**) to target ADHD, and bupropion (**3**), duloxetine (**5**) and venlafaxine (**6**) as therapies for MDD among other indications (Fig. 1).^{15,16} However, slow onset of action and a wide array of (on- and off-target) adverse effects persist with the numerous single and dual reuptake inhibitors targeting MATs in clinical use, which stipulates the continuous need for improved molecules.^{17–19}

In an attempt to discover new chemical modalities for NET, our group employed a predictive proteochemometric model to screen the Enamine REAL compound database in search for new NET inhibitors.²⁰ From this screen, a range of new and chemically diverse NET inhibitors emerged. Upon experimental validation of a subset of the newly predicted active NET inhibitors, five compounds including compound **8** (shown in Table 1) were characterized to have submicromolar potency comparable to the well-characterized NRI nisoxetine. In addition, these inhibitors complied with the typical pharmacophore of NET inhibitors for which a common binding mode can be found.²¹ This binding mode is based on several structural and computational studies which aimed to investigate the inhibitory mechanisms of reuptake inhibitors defining three different subsites within the binding pocket: one hydrophilic site which

accommodates electrostatic interactions and hydrogen bonds, and two hydrophobic pockets.^{21,22}

We selected compound **8**, a *N*,2-substituted cyclopentylamine with a NET inhibitory potency (pIC_{50}) of 7.5 ± 0.2 , as a starting point for further development of new NET inhibitors. Therefore, we designed twenty new derivatives of the compound **8**-derived *N*,2-substituted cycloalkylamine scaffold with variations aimed to optimize interactions in the aforementioned NET sub pockets. Subsequently, the compounds were evaluated on their NET inhibitory properties with the use of a label-free assay that determines transporter activity through receptor activation (TRACT).²³ Using this TRACT assay, we drafted a structure–activity relationship after which the most promising compound was resynthesized in a stereospecific manner to obtain all eight stereoisomers and subsequently determine the influence of the stereochemistry on NET inhibition. In addition, using molecular docking, the predicted binding mode was examined for two stereoisomers to elucidate similarities to existing inhibitors and to provide a structural interpretation of the observed differences in stereochemistry and insight in the key binding pocket interactions underlying the stereoselective recognition of these compounds. The structure–activity relationships detailed in this study serve as a steppingstone for further investigation of the *N*,2-substituted cycloalkylamine scaffold's potential for NET inhibition and may contribute to the improvement of current drugs available for various neurological and psychiatric disorders.

Results and discussion

Initial compound design and pharmacological characterization

Previous research conducted by Sepracor/Sunovion Pharmaceuticals Inc. (now Sumitomo Pharma Co., Ltd.) has explored the human MATs pharmacological properties and structural variations of a wide range of cycloalkylamines,²⁴ including 1,1-disubstituted derivatives.^{25,26} However, the exploration of *N*,2-substituted cycloalkylamines, such as **8** that emerged from our previous virtual screen, has not been reported. Therefore, to establish a structure–activity relationship of the *N*,2-substituted cycloalkylamine scaffold, we designed compounds with a varying cycloalkyl ring size and additional substitution on the secondary amine (compounds **9–11**), different substitution patterns on the phenyl ring (compounds **12–19**) and changes in the alkyl alcohol (compound **20–28**). The synthesis of our twenty newly designed compounds was performed at Enamine Ltd. (Kyiv, Ukraine), after which we characterized their NET inhibitory activity with an impedance-based TRACT assay.²³ This assay is based on the principle that extracellular NE is able to activate α_2 adrenergic receptors ($\alpha_2\text{AR}$) causing a cellular response, which can be measured in the xCELLigence system. NET-mediated uptake of NE, which results in lower levels of NE able to activate the receptors, influences the magnitude

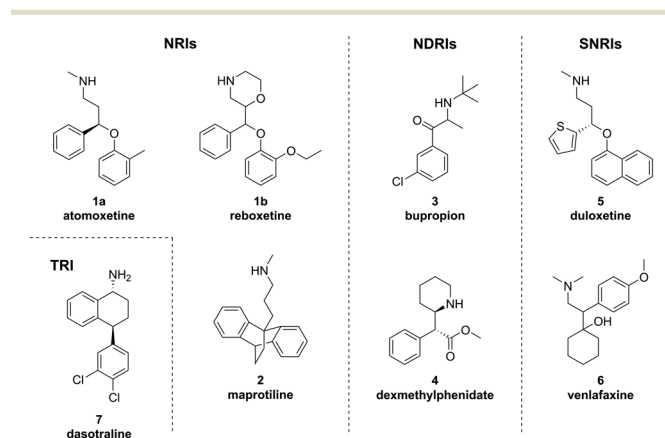


Fig. 1 Molecular structures of FDA and/or EMA approved NRIs atomoxetine (**1a**), reboxetine (**1b**) and maprotiline (**2**), NDRIs bupropion (**3**) and dexamethylphenidate (**4**), SNRIs duloxetine (**5**) and venlafaxine (**6**), and discontinued triple reuptake inhibitor (TRI) dasotraline (**7**).

Table 1 Inhibitory potency values or percentage enhancement at 1 μ M of reference inhibitors nisoxetine and compound **8**, and cycloalkylamine derivatives **1–20** in HEK293–Jumpln–NET cells determined with NET TRACT assay

Cmpd	<i>n</i>	<i>R</i> ¹	<i>R</i> ²	<i>R</i> ³	% enhancement \pm SD ^a at 1 μ M	pIC ₅₀ \pm SEM ^b (IC ₅₀ (nM))
Nisoxetine						8.2 \pm 0.0 (6.1)
8	1	H		3,4-diCl	N.D.	7.5 \pm 0.2 (32) ^c
9	1	CH ₃		3,4-diCl	48 \pm 3%	N.D.
10	0	H		3,4-diCl	50 \pm 29%	N.D.
11	2	H		3,4-diCl	70 \pm 17%	6.3 \pm 0.1 (524)
12	1	H		H	−5 \pm 14%	N.D.
13	1	H		2-Cl	−4 \pm 6%	N.D.
14	1	H		3-Cl	18 \pm 7%	N.D.
15	1	H		4-Cl	59 \pm 21%	N.D.
16	1	H		3-CF ₃ , 4-Cl	13 \pm 9%	N.D.
17	1	H		2-OEt	−12 \pm 15%	N.D.
18	1	H		3-OEt	−9 \pm 11%	N.D.
19	1	H			92 \pm 5%	7.3 \pm 0.2 (45)
20	1	H		3,4-diCl	97 \pm 2%	7.1 \pm 0.2 (88)
21	1	H	H	3,4-diCl	65 \pm 5%	N.D.
22	1	H		3,4-diCl	79 \pm 3%	6.6 \pm 0.1 (235)
23	1	H		3,4-diCl	85 \pm 1%	7.0 \pm 0.0 (97)
24	1	H		3,4-diCl	87 \pm 1%	6.6 \pm 0.2 (236)
25	1	H		3,4-diCl	83 \pm 8%	6.5 \pm 0.1 (338)
26	1	H		3,4-diCl	92 \pm 19%	6.8 \pm 0.3 (173)
27	1	H		3,4-diCl	106 \pm 12%	8.3 \pm 0.0 (5.4)
28	1	H		3,4-diCl	69 \pm 4%	6.2 \pm 0.0 (605)

^a Percentage enhancement represents the magnitude of potentiating the NE-induced response compared to nisoxetine (100%). Values are shown as mean \pm SD of two independent experiments performed in duplicate. ^b pIC₅₀ values are presented as mean \pm SEM of three independent experiments performed in duplicate. ^c pIC₅₀ value obtained from Bongers *et al.* (2023)²⁰ using the same assay. N.D. is not determined.

of this response. Consequently, NET inhibition will result in an enhanced cellular response. All compounds were screened for their inhibitory capacity (shown as percentage enhancement of the NE-induced response at 1 μ M) in HEK293 cells with doxycycline-inducible expression of NET and endogenous expression of the α_2 AR. Subsequently, if more than 70% enhancement was observed compared to NRI nisoxetine at 100%, compounds were further characterization in full concentration–inhibition curves to determine their inhibitory potency (pIC₅₀) (Table 1).

Nisoxetine displayed high potency for NET (pIC₅₀ of 8.2 \pm 0.0) corresponding to values previously found by our group and those reported in literature.^{23,27} Substituting the

secondary amine of **8** with a methyl group (**9**) to produce a tertiary amine reduced the inhibitory potency from 7.5 \pm 0.2 to less than 50% enhancement at 1 μ M. In contrast, the introduction of a tertiary amine for existing triple reuptake inhibitors reported in literature often increased the potency towards the serotonin transporter (SERT) compared to the NET and dopamine transporter (DAT), in addition to the general trend of decreased microsomal stability.²⁸ Decreasing the cycloalkyl ring with one carbon atom to cyclobutyl (**10**) resulted in diminished enhancement similar to **9** whereas expanding the ring to a cyclohexyl resulted in a pIC₅₀ value of 6.3 \pm 0.1 for compound **11**. A similar range of cycloalkyl moieties was introduced in the series of 1,1-disubstituted

cycloalkylmethanamines from Sunovion Pharmaceuticals Inc., which led to a different trend in NET inhibition where the cyclohexyl ring displayed the highest potency, followed by the cyclobutyl ring and thereafter the cyclopentyl ring.²⁵ Alterations made in the dichloro-substitution pattern of the aromatic ring (compounds **12–18**, including ethoxy substitutions to mimic existing NRIs such as reboxetine and viloxazine) fully abrogated NET inhibitory activity except for the *para*-chloro substituted compound **15** which still enhanced the NE-induced effect at 1 μ M (60%). This phenomenon was also observed for a series of piperidine-based triple reuptake inhibitors (TRIs) from Takeda Pharmaceutical Company Ltd., where the substitution of the 3,4-dichloro pattern to other halogen patterns (such as 3-Cl, 4-Cl and 3-Cl, 4-F) greatly decreased the inhibitory potency.²⁹ On the contrary, completely substituting the 3,4-dichlorophenyl ring with a 2-naphthyl moiety (**19**) resulted in submicromolar inhibition of NET (pIC_{50} of 7.3 ± 0.2) similar to **8**. Many studies on the design of new dual and triple reuptake inhibitors reported the 2-naphthyl and 3,4-dichlorophenyl moieties as favored substitution patterns to occupy one of the aforementioned hydrophobic subpockets in MATs resulting in potent inhibition next to good oral bioavailability, metabolic stability and brain penetration.^{28,30,31} While it has been proposed that increasing the hydrophobicity of the substituted phenyl ring in NRIs and NDRIs may reduce the addictiveness of ADHD drugs, in the case of NET, none of the clinically used therapeutics so far contains such a moiety.^{32,33}

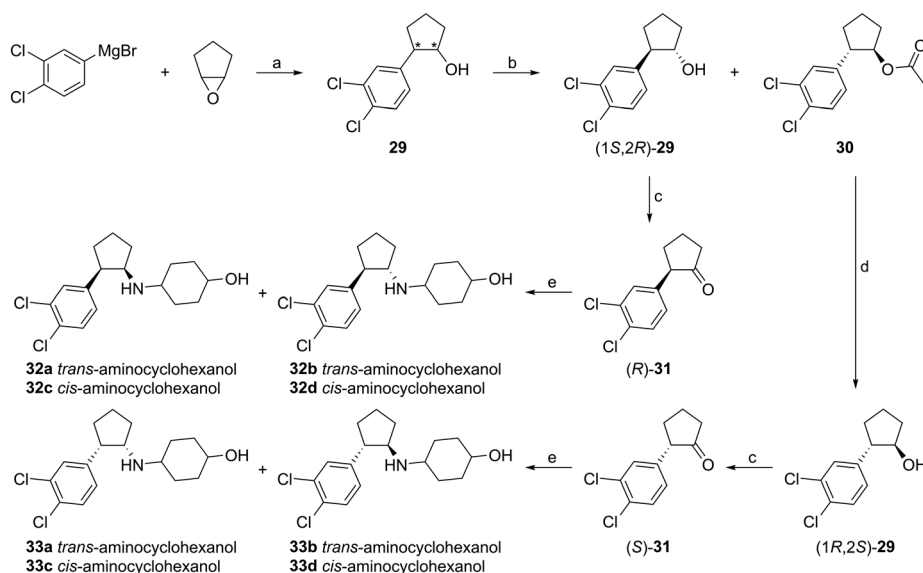
Lastly, to explore the available space surrounding the butyl alcohol as well as the potential hydrogen-bond formation of its hydroxyl, the moiety was altered in various ways. Removal of the butyl alcohol, resulting in primary amine **21**, significantly reduced the inhibitory effect at 1 μ M compared to nisoxetine, which is in line with previous findings of cycloalkylmethanamines as well as the successive series of cycloalkylethanamines and dasotraline derivatives in which the conversion of the tertiary amine to a primary amine with removal of both methyl substituents diminished NET inhibition by at least 45-fold and 70-fold, respectively.^{25,26,34} Conversely, all other changes in the butyl alcohol chains were tolerated, with compounds **22–26** and **28** displaying submicromolar NET activity, albeit with a 3- to 20-fold reduced inhibitory potency compared to compound **8** (Table 1). Interestingly, complete removal of the hydroxyl (**22**) or replacing it with a bulky phenoxy (**24**) or methylamine (**25**) similarly reduced potency by 8-fold (Table 1), suggesting that disrupted H-bond interaction with the hydroxyl-group is harmful for NET inhibition. On the other hand, substitution of the butyl alcohol with a more rigid cyclohexanol (**27**) resulted in the best NET inhibitor (pIC_{50} of 8.3 ± 0.0) with similar activity to reference compound nisoxetine and a 6.3-fold increased inhibitory potency compared to parent compound **8** (Table 1).

Follow-up synthesis and pharmacological characterization

As reported for many marketed drugs, amongst which several MAT inhibitors, administration of a single stereoisomer can substantially improve efficacy and safety compared its racemic or diastereomeric mixtures.^{35–37} This is exemplified with NRI viloxazine, in which the *S*(-)-enantiomer is five times more potent than the *R*(+)-enantiomer,³⁸ and reboxetine, where *S,S*(+)-reboxetine has a 130-fold higher inhibitory activity for NET compared to the *R,R*(-)-reboxetine analogue.³⁹ Hence, the most promising inhibitor, compound **27**, was selected for further investigation regarding stereochemistry since it was originally tested as a mixture of stereoisomers (ESI[†]). Considering the two chiral carbons on the cyclopentyl ring and the *cis-trans* isomerism of the cyclohexyl ring, eight stereoisomers exist. All eight were separately obtained through the synthetic approach outlined in Scheme 1.

The synthesis started with the nucleophilic ring opening of 1,2-epoxycyclopentane using Grignard reagent 3,4-dichlorophenylmagnesium bromide to obtain a racemic mixture of the *trans*-isomers of **29**. Subsequently, with the use of immobilized *Candida antarctica* lipase B the *R*-alcohol was enantioselectively acetylated in the presence of vinyl acetate.⁴⁰ The formed acetate (**30**) was separated from (1*S*,2*R*)-**29** and easily hydrolyzed to obtain alcohol (1*R*,2*S*)-**29**, a stereospecific approach previously reported for the synthesis of cyclopentyl sulfonamides targeting AMPA receptors.⁴¹ With both *trans*-oriented enantiomers a Dess–Martin oxidation of the alcohol yielded cyclopentanones (*R*)-**31** and (*S*)-**31**, each with one defined stereocenter, as confirmed by specific optical rotation measurements of (*R*)-**31** and (*S*)-**31**. Subsequent reductive amination of intermediates (*R*)-**31** and (*S*)-**31** with *trans*- or *cis*-4-aminocyclohexanol and sodium cyanoborohydride led to the formation of two products, as evidenced by NMR and LC-MS analyses matching the final product's exact mass. This suggested that both *cis*- and *trans*-configurations of the cyclopentyl were generated from (*R*)-**31** and (*S*)-**31**, respectively, through hydride donation on each side of the iminium ion during reductive amination. The two diastereomers in each reaction mixture were separated using flash column chromatography providing all eight stereoisomers of original compound **27** as final compounds **32a–32d** and **33a–33d**. The relative configuration of the cyclopentyl was determined with the use of 2D NMR (ESI[†]) and in combination with the defined stereocenter of intermediates (*R*)-**31** and (*S*)-**31**, the absolute configurations of **32a–32d** and **33a–33d** were assigned.

To determine the most active stereoisomer, all eight synthesized compounds **32a–32d** and **33a–33d** were characterized in the NET TRACT assay (Table 2 and Fig. 2). Interestingly, most stereoisomers displayed a NET inhibitory potency that was similar to the mixture (**27**), except for **32a**, **32c** and **33c**, exemplified with a rightward shift of the inhibition curve for **32a** compared to **32b** as a result of the



Scheme 1 Synthesis of all eight stereoisomers 31a–31d and 32a–32d of compound 27. Reagents and conditions: a) cat. Cu^{I} , THF, rt, 21 h, 82%; b) *Candida antarctica* lipase B, vinyl acetate, MBTE, rt, 17 h, 90% ((1S,2R)-28), 94% (29); c) Dess–Martin periodinane, DCM, 0 °C, 5–18 h, 94–95%; d) K_2CO_3 , MeOH, rt, 18 h, 97%; e) *trans*-4-aminocyclohexanol or *cis*-4-aminocyclohexanol, NaBH_3CN , AcOH, MeOH, rt or 60 °C, 3–5 days, 3–39%. Asterisks denominate chiral centers.

cyclopentyl ring orientation (Fig. 2a, Table 2). This rightward shift of the curve indicates that a *trans*-orientation of the cyclopentyl stereocenters is favorable compared to the *cis*-orientation which was similarly observed for diastereomers 33a and 33b (Table 2). In addition, no apparent potency shift could be observed for compounds 33b and 33d with a *trans*- or *cis*-aminocyclohexanol, respectively (Fig. 2b).

The absence of a potency shift was observed for all diastereomeric pairs (32a vs. 32c, 32b vs. 32d, 33a vs. 33c and 33b vs. 33d), which contain the same configuration of the cyclopentyl stereochemistry but a different configuration of the aminocyclohexanol (Table 2). Additionally, comparison of enantiomers 32b vs. 33b and 32d vs. 33d, indicated that there is no distinct difference between the single enantiomers for each pair bearing a *trans*-oriented cyclopentyl ring (Table 2). We confirmed that the observed effects in the label-free TRACT assay were indeed due to NET inhibition as 33b obtained similar inhibitory potency values (pIC_{50} of 8.4 ± 0.1 for both assay types) in an orthogonal fluorescent neurotransmitter uptake assay (ESI,† Fig. S1).

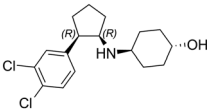
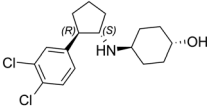
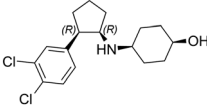
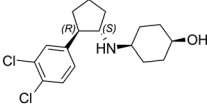
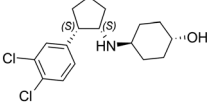
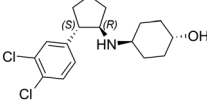
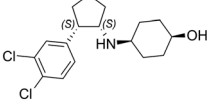
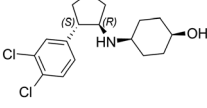
Although the absolute conformation of the 3,4-dichlorophenyl ring and amine substitution on the cyclopentyl ring showed minimal influence on the activity of compound 27 stereoisomers, previous studies of dasotraline (Fig. 1) derivatives have revealed a trend for the 3,4-dichlorophenyl moiety with a preference for (*S*)- over (*R*)-configuration.³⁴ Recent studies have examined the structure–activity relationship of modafinil-based DRIs, with a focus on chirality.⁴² It was shown that the two enantiomers, compounds 7 h and 8 h, exhibited opposite selectivity profiles *in vitro*, despite both having submicromolar potency for DAT. Interestingly, the *in vivo* activity was inversely related

to their individual IC_{50} values, highlighting the crucial role of chirality in MAT inhibitors.

Computational characterization

To provide insight into the structural determinants of stereoselective recognition, we used molecular docking of the most (33b) and least (32a) potent compounds in a computational model of the human NET from AlphaFold 2. Of note: we have aligned our model with a recent cryo-EM structure of the human NET⁴³ and found good overlap (RMSD of 1.01 Å) with our model (ESI,† Fig. S2). For this purpose, the putative binding site was extracted from previous studies which identified D75 as a key residue.²¹ The predicted binding site was found in the transmembrane region (Fig. 3a), close to two sodium ions and a chloride ion. We observed a similar recognition pattern for both inhibitors (Fig. 3b), where the 3,4-dichlorophenyl group binds deeply into the hydrophobic pocket. This pocket has previously been predicted to accommodate 3,4-dichlorophenyl groups as well as naphthyl groups of various MAT inhibitors.⁴⁴ Moreover, the canonical ionic interaction for substrate and inhibitor recognition is observed with the conserved D75 and the protonated amines in both compounds.^{21,45} In addition, a hydrogen bond is formed between D473 and the compounds' hydroxyl substituent. Even though this residue has not formerly been described to directly influence binding of NRIs with the exemption of nisoxetine,^{46,47} it is directly involved in the conserved transmembrane domain TM1–TM10 interaction by salt bridge formation with R81, likewise observed for the other monoamine transporters and their bacterial homologue LeuT with their corresponding residues.^{48,49} It is hypothesized that these so-called 'gating

Table 2 Inhibitory potency values of stereoisomers **32a–32d** and **33a–33d** determined with NET TRACT assay in HEK293-JumpIn-NET cells

Cmpd	Molecular structure	pIC ₅₀ ± SEM ^a (IC ₅₀ (nM))
32a		7.1 ± 0.3 (73)***
32b		8.3 ± 0.1 (4.5)
32c		7.5 ± 0.2 (35)**
32d		8.1 ± 0.0 (7.8)
33a		7.8 ± 0.1 (14)
33b		8.4 ± 0.1 (4.3)
33c		7.7 ± 0.1 (19)*
33d		8.3 ± 0.2 (4.5)

^a Values represent mean ± SEM of at least three independent experiments performed in duplicate. One-way ANOVA with Dunnett's *post hoc* test was used to analyze differences in pIC₅₀ compared to compound 27 (**p* < 0.05, ***p* < 0.01, ****p* < 0.001).

residues' in the extracellular gate are crucial in shielding the substrate from the extracellular side as part of the translocation mechanism to the cytosol. On the other hand, a clear difference was observed between the two stereoisomers in the accommodation of the cyclopentyl ring, which was predicted to reside in a largely hydrophilic region for compound **32a** (red, Fig. 3b). Conversely, the predicted binding mode of **33b** did not show this angle for the cyclopentyl moiety which may rationalize the loss in inhibitory potency from **33b** to **32a**.

Conclusions

In the present study, we explored the *N*,2-substituted cycloalkylamine scaffold to yield inhibitors for the human NET. Twenty new derivatives were designed, synthesized and evaluated for their inhibitory properties using a label-

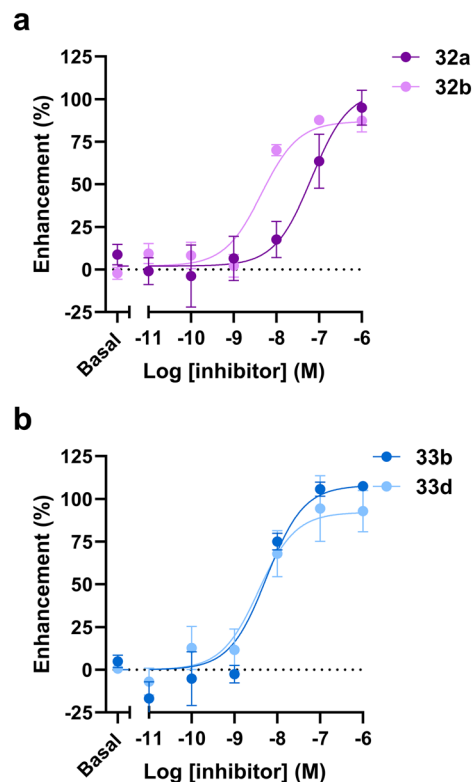


Fig. 2 (a) Concentration–inhibition curves of inhibitors **32a**, **32b** with a (1*R*,2*R*)- and (1*S*,2*R*)-cyclopentyl orientation, respectively, and (b) **33b**, **33d** with a *trans*- and *cis*-aminocyclohexanol orientation, respectively, in the NET TRACT assay. Cells are pretreated for 1 h with vehicle or one of six increasing concentrations of inhibitor, then stimulated with 1 μM NE or vehicle. NE-induced cellular response is shown as percentage enhancement. Data were normalized to the average top and bottom values of the nisoxetine concentration–inhibition curve. Data are shown as mean ± SEM of three to four individual experiments performed in duplicate.

free impedance-based TRACT assay. The eleven compounds that showed over 70% enhancement at 1 μM of a NET inhibitory effect compared to nisoxetine (100%) were fully characterized providing submicromolar potencies. Compound 27 bearing a cyclohexanol ring, emerged as the lead compound with a pIC₅₀ value of 8.3 ± 0.1 similar to reference inhibitor nisoxetine. The main emphasis of the current study was on the subsequent synthesis of all eight possible stereoisomers of 27, for which we used a bioorganic approach. Subsequently we evaluated their inhibitory potency in the TRACT assay resulting in pIC₅₀ values between 7.1 ± 0.3 and 8.4 ± 0.1, showing a preference for the *trans*-oriented cyclopentyl ring. Additionally, computational docking predicted a similar binding mode to other MAT inhibitors and revealed several key interactions including a hydrogen bond with gating residue D473. This research introduces NET inhibitors with nanomolar affinity, where stereochemistry is a key factor influencing the orientation in the NET binding pocket. These results provide valuable perspectives for monoamine transport-targeting treatments including

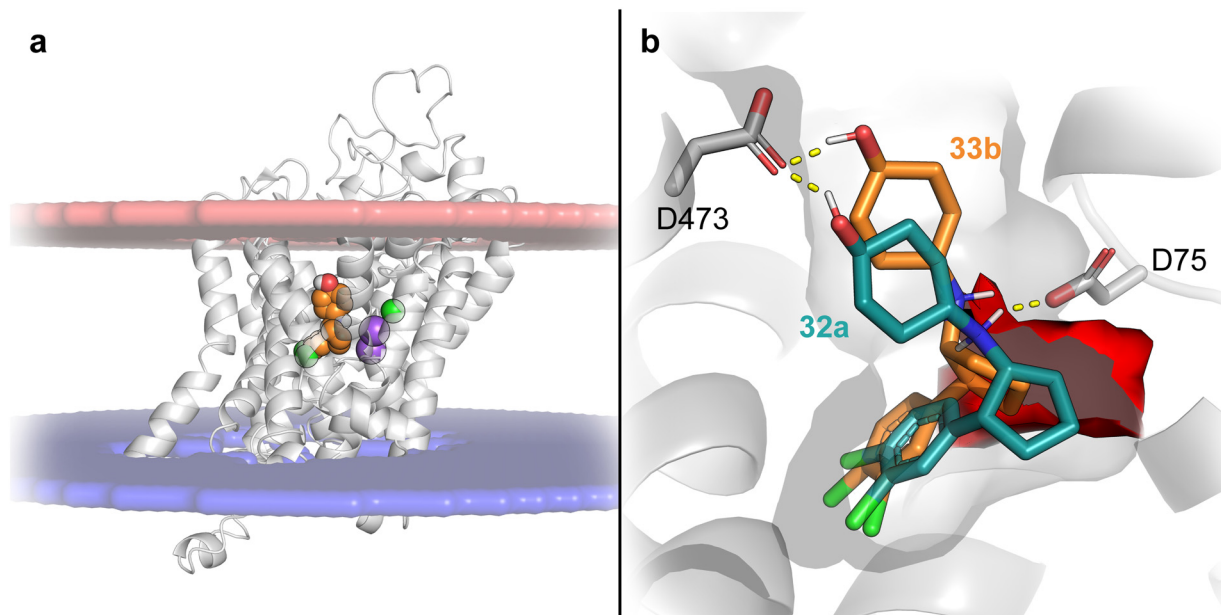


Fig. 3 (a) Predicted orientation of the NET AlphaFold model in the plasma membrane in spheres. Extracellular side in red and cytoplasmic side in blue. Orange spheres represent **33b**, sodium and chloride ions are represented in purple and green spheres, respectively. (b) Predicted binding orientation of most potent (**33b**) and least potent (**32a**) stereoisomers in orange and cyan, respectively. Both compounds show an ionic interaction with D75 and an additional interaction with D473. The red surface represents a hydrophilic region of the binding site predicted by SiteMap. For visualization purposes, the sodium and chloride ions are not displayed.

closely related and clinically relevant transporters such as DAT and SERT.

Experimental

General chemistry

All solvents and reagents were purchased from commercial sources and were of analytical grade. Compounds **8–27** were obtained from Enamine Ltd. (Kyiv, Ukraine). Demineralized water is referred to as H₂O and was used in all cases unless noted otherwise (*i.e.*, brine). All reactions were routinely monitored with thin-layer chromatography (TLC), using aluminum silica gel coated 60 F₂₅₄ plates from Merck (Darmstadt, Germany) and visualized by UV irradiation at 254 nm and subsequent staining with ceric ammonium molybdate, KMnO₄ or ninhydrin solution. Purification by flash column chromatography was carried out with the use of silica gel irregular ZEOPrep® particles (60–200 µm) from VWR (Amsterdam, The Netherlands) or by using a Selekt automatic flash chromatography system from Biotage® (Uppsala, Sweden) with pre-packed cartridges (Biotage® Sfär C18 D Duo 100 Å 30 µm (C18)). Solutions were concentrated using a Heidolph (Schwabach, Germany) Hei-VAP Value rotary evaporator. Nuclear magnetic resonance (NMR) spectra were recorded on a Bruker (Billerica, MA, USA) AV-400 liquid or AV-400 WB spectrometer (¹H NMR, 400 MHz and ¹³C NMR, 101 MHz) at ambient temperature and subsequently analyzed with MestReNova v14.1.0 software (Mestrelab Research S.L., Santiago de Compostela, Spain). Chemical shifts are reported in parts per million (ppm), designated by

δ and corrected to the internal standard tetramethylsilane (δ = 0). Multiplicities are indicated by s, singlet; d, doublet; dd, doublet of doublets; td, triplet of doublets; dtd, doublet of triplet of doublets; t, triplet; dt, doublet of triplets; tt, triplet of triplets; ddt, doublet of doublet of triplets; q, quartet; m, multiplet; br s, broad singlet. Coupling-constants (*J*) are reported in Hz. Specific optical rotations ($[\alpha]_D$) were measured with a modular compact polarimeter 100 (MCP 100) from Anton Paar GmbH (Graz, Austria) at 589 nm. Mass and compound purity analyses were performed with liquid chromatography-mass spectrometry (LC-MS) using a LCMS-2020 system from Shimadzu (Kyoto, Japan) coupled to a Phenomenex Gemini® C18 110 Å column (50 mm × 3 mm × 3 µm). Samples were prepared by dissolving 0.3–0.8 mg of compound in 1 mL of a 1 : 1 : 1 mixture of CH₃CN/H₂O/*t*BuOH and were eluted using an isocratic system of H₂O/CH₃CN with 0.1% FA, using gradients from 100 : 0 to 60 : 40 and 90 : 10 to 10 : 90 in an elution time of 15 minutes. All tested compounds were determined to be of >95% purity as determined by HPLC measuring UV absorption at 215 nm.

Synthetic procedures

2-(3,4-Dichlorophenyl)cyclopentan-1-ol (29). A solution (0.5 M) of (3,4-dichlorophenyl)magnesium bromide (40.0 mL, 20.0 mmol, 1.0 equiv.) in THF was added to a flame-dried flask charged with copper(I) iodide (267 mg, 1.40 mmol, 0.07 equiv.). Subsequently, a solution of cyclopentene oxide (1.73 mL, 20.0 mmol, 1.0 equiv.) in THF (40 mL) was added dropwise over a period of 30 minutes. The mixture was

allowed to stir at rt for 21 h and monitored on TLC with ceric ammonium molybdate staining. Upon completion, the mixture was quenched with sat. NH_4Cl solution (80 mL) followed by extraction with diethyl ether (100 mL) and separation of the organic phase. The aqueous phase was extracted with ether (60 mL). The combined organic phases were washed with sat. NH_4Cl solution (60 mL), dried over MgSO_4 , filtrated and concentrated *in vacuo*. Flash column chromatography on silica gel using a gradient of 40 to 100% DCM in PE as mobile phase provided intermediate compound **29**. Yellow oil (3.79 g, 16.4 mmol, 82%). ^1H NMR (400 MHz, CDCl_3) δ 7.35 (d, J = 8.3 Hz, 1H), 7.33 (d, J = 2.1 Hz, 1H), 7.08 (dd, J = 8.3, 2.1 Hz, 1H), 4.05 (q, J = 6.3, 5.4 Hz, 1H), 2.80 (dt, J = 10.1, 7.8 Hz, 1H), 2.18–2.02 (m, 3H), 1.90–1.72 (m, 2H), 1.71–1.59 (m, 2H). HPLC t_R : 10.736 min.

(1S,2R)-2-(3,4-Dichlorophenyl)cyclopentan-1-ol ((1S,2R)-29) and (1R,2S)-2-(3,4-dichlorophenyl)cyclopentyl acetate (30). To a stirred solution of intermediate **29** (2.03 g, 8.78 mmol, 1.0 equiv.) in MBTE (43.9 mL) was added 1.00 g of *Candida antarctica* lipase B immobilized on Immobead 150 (recombinant from yeast, ≥ 2000 U g^{-1}) followed by the addition of vinyl acetate (4.07 mL, 43.9 mmol, 5.0 equiv.). The mixture was stirred at rt for 17 h monitored by LC-MS after which the suspension was filtrated and concentrated *in vacuo*. Flash column chromatography on silica gel using a gradient of 30 to 80% DCM in PE as mobile phase provided intermediates **(1S,2R)-29** and **30**. Intermediate **(1S,2R)-29**: transparent oil (916 mg, 3.96 mmol, 90%). ^1H NMR (400 MHz, CDCl_3) δ 7.32 (d, J = 8.2 Hz, 1H), 7.30 (d, J = 2.1 Hz, 1H), 7.03 (dd, J = 8.3, 2.1 Hz, 1H), 3.91 (q, J = 7.4 Hz, 1H), 2.99 (br s, 1H), 2.72 (dt, J = 10.2, 7.9 Hz, 1H), 2.14–2.03 (m, 1H), 2.03–1.93 (m, 1H), 1.87–1.66 (m, 2H), 1.66–1.49 (m, 2H). HPLC t_R : 10.719 min. Intermediate **30**: transparent oil (1.13 g, 4.14 mmol, 94%). ^1H NMR (400 MHz, CDCl_3) δ 7.35–7.30 (m, 2H), 7.07 (dd, J = 8.3, 2.1 Hz, 1H), 5.03 (td, J = 7.0, 5.0 Hz, 1H), 3.09 (dt, J = 9.7, 7.6 Hz, 1H), 2.21–2.10 (m, 2H), 2.00 (s, 3H), 1.88–1.78 (m, 2H), 1.75–1.60 (m, 2H). HPLC t_R : 12.223 min.

(1R,2S)-2-(3,4-dichlorophenyl)cyclopentan-1-ol ((1R,2S)-29). A suspension of **30** (2.03 g, 7.45 mmol, 1.0 equiv.) and potassium carbonate (3.09 g, 22.4 mmol, 3.0 equiv.) in MeOH (37.2 mL) was stirred at rt for 18 h. The solvent was removed *in vacuo*, the remaining residue was dissolved in water (50 mL) and extracted twice with ethyl acetate (30 mL). The combined organic layers were washed with brine (30 mL), dried over MgSO_4 , followed by concentration *in vacuo* to provide intermediate **(1R,2S)-29**. Transparent oil (1.69 g, 7.33 mmol, 98%). ^1H NMR (400 MHz, CDCl_3) δ 7.30 (d, J = 8.3 Hz, 1H), 7.28 (d, J = 2.1 Hz, 1H), 7.01 (dd, J = 8.3, 2.1 Hz, 1H), 3.84 (q, J = 7.3 Hz, 1H), 3.37 (br s, 1H), 2.67 (dt, J = 10.2, 7.8 Hz, 1H), 2.05 (dtd, J = 12.5, 7.9, 4.0 Hz, 1H), 2.00–1.89 (m, 1H), 1.83–1.64 (m, 2H), 1.64–1.54 (m, 1H), 1.54–1.45 (m, 1H). HPLC t_R : 10.706 min.

General procedure A. Intermediate **(1S,2R)-29** or **(1R,2S)-29** (1.0 equiv.) was dissolved in DCM (0.2 M) and allowed to cool

down to 0 °C after which Dess–Martin periodinane (1.2 equiv.) was added. The mixture was warmed up to rt and stirred for 5 h followed by dilution with DCM. After quenching with 1 N NaOH, the organic phase was separated, dried over MgSO_4 , filtrated and concentrated *in vacuo*. Flash column chromatography on silica gel using a gradient of 50 to 80% DCM in PE as mobile phase provided intermediates **(R)-31** and **(S)-31**.

(R)-2-(3,4-Dichlorophenyl)cyclopentan-1-one ((R)-31).

Intermediate **(R)-31** was obtained from intermediate **(1S,2R)-29** following general procedure A. Yellow oil (472 mg, 2.06 mmol, 95%). ^1H NMR (400 MHz, CDCl_3) δ 7.36 (d, J = 8.3 Hz, 1H), 7.28 (dd, J = 2.1, 0.6 Hz, 1H), 7.03 (dd, J = 8.3, 2.1 Hz, 1H), 3.31–3.18 (m, 1H), 2.52–2.37 (m, 2H), 2.31–2.17 (m, 1H), 2.19–2.07 (m, 1H), 2.09–1.93 (m, 1H), 1.96–1.81 (m, 1H). $[\alpha]_D^{25} = +27.050^\circ$ (c = 2.0, CHCl_3). HPLC t_R : 11.152 min.

(S)-2-(3,4-Dichlorophenyl)cyclopentan-1-one ((S)-31).

Intermediate **(S)-31** was obtained from intermediate **(1R,2S)-29** following general procedure A. Yellow oil (793 mg, 3.46 mmol, 94%). ^1H NMR (400 MHz, CDCl_3) δ 7.36 (d, J = 8.2 Hz, 1H), 7.28 (d, J = 2.2 Hz, 1H), 7.03 (dd, J = 8.3, 2.2 Hz, 1H), 3.31–3.19 (m, 1H), 2.52–2.38 (m, 2H), 2.31–2.19 (m, 1H), 2.18–2.09 (m, 1H), 2.09–1.95 (m, 1H), 1.95–1.83 (m, 1H). $[\alpha]_D^{25} = -35.600^\circ$ (c = 2.0, CHCl_3). HPLC t_R : 10.894 min.

General procedure B. Intermediate **(R)-31** or **(S)-31** (1.0 equiv.) and *cis*-4-aminohexan-1-ol hydrochloride or *trans*-4-aminocyclohexan-1-ol (3.0 equiv.) were dissolved in MeOH (0.2 M) after which acetic acid (2.0 or 3.0 equiv.) and NaBH_3CN (4.0 equiv.) were added. The reaction mixture was stirred at rt or 60 °C for 3 to 5 days while routinely monitoring the pH and reaction progress on TLC. The reaction was stopped by solvent removal *in vacuo* followed by the addition of DCM and 1 N aqueous NaOH. The aqueous phase was washed twice with DCM after which the combined organic phases were dried over MgSO_4 and concentrated *in vacuo*. Automatic column chromatography was used to purify the combination of formed diastereomers after which flash column chromatography was used to separate the two diastereomers formed in each reaction to give final compounds **32a–32d** and **33a–33d**.

***trans*-4-(((1R,2R)-2-(3,4-Dichlorophenyl)cyclopentyl)amino)cyclohexan-1-ol (32a).** Final compounds **32a** and **32b** were obtained from intermediate **(R)-31** and *trans*-4-aminocyclohexanol following general procedure B at rt. Automatic column chromatography (C18) with 0 to 60% CH_3CN in H_2O + 0.1% TFA as mobile phase on Biotage® Selekt. Transparent oil (33.2 mg, 0.10 mmol, 14%). ^1H NMR (400 MHz, CDCl_3) δ 7.36 (d, J = 8.2 Hz, 1H), 7.32 (d, J = 2.1 Hz, 1H), 7.06 (dd, J = 8.2, 2.1 Hz, 1H), 3.52 (tt, J = 10.7, 4.3 Hz, 1H), 3.37 (q, J = 6.0 Hz, 1H), 3.15 (q, J = 7.4 Hz, 1H), 2.23 (tt, J = 10.9, 3.8 Hz, 1H), 2.09–1.79 (m, 7H), 1.77–1.48 (m, 3H), 1.31–1.09 (m, 4H), 1.07–0.80 (m, 2H). ^{13}C NMR (101 MHz, CDCl_3) δ 142.5, 132.2, 130.8, 130.1, 130.1, 128.3, 70.6, 59.7, 54.1, 48.4, 34.2, 34.2, 32.5, 31.9, 31.1, 29.4, 22.2. LC-MS (ESI+) m/z calcd. for $\text{C}_{17}\text{H}_{23}\text{Cl}_2\text{NO}$ $[(M + H)]^+$: 328.12; found: 328.05. HPLC t_R : 8.526 min.

***trans*-4-(((1*S*,2*R*)-2-(3,4-Dichlorophenyl)cyclopentyl)amino)cyclohexan-1-ol (32b).** White solid (18.0 mg, 0.06 mmol, 7%). ^1H NMR (400 MHz, CDCl_3) δ 7.36 (d, J = 8.2 Hz, 1H), 7.33 (d, J = 2.1 Hz, 1H), 7.08 (dd, J = 8.2, 2.1 Hz, 1H), 3.54 (tt, J = 10.7, 4.2 Hz, 1H), 3.14 (q, J = 8.1 Hz, 1H), 2.65 (q, J = 9.2 Hz, 1H), 2.36 (tt, J = 10.8, 3.7 Hz, 1H), 2.15–2.04 (m, 2H), 1.97–1.72 (m, 6H), 1.62 (ddt, J = 12.8, 10.2, 8.6 Hz, 1H), 1.54–1.32 (m, 3H), 1.28–1.15 (m, 2H), 1.12–1.00 (m, 1H), 0.98–0.85 (m, 1H). ^{13}C NMR (101 MHz, CDCl_3) δ 145.0, 132.5, 130.5, 130.2, 129.5, 127.0, 70.5, 63.9, 54.6, 52.8, 34.3, 34.2, 33.8, 33.6, 32.3, 31.3, 22.9. LC-MS (ESI+) m/z calcd. for $\text{C}_{17}\text{H}_{23}\text{Cl}_2\text{NO}$ $[(\text{M} + \text{H})]^+$: 328.12; found: 328.05. HPLC t_R : 8.744 min.

***cis*-4-(((1*R*,2*R*)-2-(3,4-Dichlorophenyl)cyclopentyl)amino)cyclohexan-1-ol (32c).** Final compound 32c and 32d were obtained from intermediate (*R*)-31 and *cis*-4-aminocyclohexanol hydrochloride following general procedure B at 60 °C. Column chromatography on silica gel with 4 to 10% MeOH in DCM as mobile phase. Off-white solid (8.4 mg, 0.03 mmol, 3%). ^1H NMR (400 MHz, CDCl_3) δ 7.36 (d, J = 8.3 Hz, 1H), 7.34 (d, J = 2.1 Hz, 1H), 7.09 (dd, J = 8.3, 2.1 Hz, 1H), 3.84–3.75 (m, 1H), 3.38 (q, J = 5.7 Hz, 1H), 3.14 (q, J = 7.4, 6.5 Hz, 1H), 2.40–2.28 (m, 1H), 2.05–1.85 (m, 4H), 1.76–1.15 (m, 12H). ^{13}C NMR (101 MHz, CDCl_3) δ 142.5, 132.2, 130.8, 130.1, 130.0, 128.3, 67.2, 59.3, 52.6, 48.6, 32.5, 31.3, 31.3, 29.3, 28.4, 27.4, 22.2. LC-MS (ESI+) m/z calcd. for $\text{C}_{17}\text{H}_{23}\text{Cl}_2\text{NO}$ $[(\text{M} + \text{H})]^+$: 328.12; found: 328.05. HPLC t_R : 8.847 min.

***cis*-4-(((1*S*,2*R*)-2-(3,4-Dichlorophenyl)cyclopentyl)amino)cyclohexan-1-ol (32d).** Transparent oil (55.5 mg, 0.17 mmol, 27%). ^1H NMR (400 MHz, CDCl_3) δ 7.40–7.33 (m, 2H), 7.10 (dd, J = 8.3, 2.1 Hz, 1H), 3.86–3.78 (m, 1H), 3.21 (q, J = 8.1 Hz, 1H), 2.79 (q, J = 8.9 Hz, 1H), 2.64 (s, 2H), 2.55–2.47 (m, 1H), 2.19–2.04 (m, 2H), 1.91–1.72 (m, 2H), 1.69–1.35 (m, 10H). ^{13}C NMR (101 MHz, CDCl_3) δ 144.7, 132.5, 130.5, 130.2, 129.4, 127.0, 66.4, 63.1, 53.5, 52.0, 34.0, 33.0, 31.2, 31.1, 27.8, 26.8, 23.0. LC-MS (ESI+) m/z calcd. for $\text{C}_{17}\text{H}_{23}\text{Cl}_2\text{NO}$ $[(\text{M} + \text{H})]^+$: 328.12; found: 328.05. HPLC t_R : 9.152 min.

***trans*-4-(((1*S*,2*S*)-2-(3,4-Dichlorophenyl)cyclopentyl)amino)cyclohexan-1-ol (33a).** Final compound 33a and 33b were obtained from intermediate (*S*)-31 and *trans*-4-aminocyclohexanol following general procedure B at rt. Automatic column chromatography (C18) with 0 to 60% CH_3CN in H_2O + 0.1% TFA as mobile phase on Biotage® Selekt followed by column chromatography on silica gel with 4 to 10% MeOH in DCM as mobile phase. Off-white solid (106 mg, 0.32 mmol, 39%). ^1H NMR (400 MHz, CDCl_3) δ 7.36 (d, J = 8.3 Hz, 1H), 7.31 (d, J = 2.1 Hz, 1H), 7.06 (dd, J = 8.3, 2.1 Hz, 1H), 3.49 (tt, J = 10.8, 4.2 Hz, 1H), 3.37 (q, J = 6.0 Hz, 1H), 3.16 (q, J = 7.2 Hz, 1H), 2.23 (tt, J = 10.8, 3.8 Hz, 1H), 2.08–1.78 (m, 7H), 1.76–1.44 (m, 5H), 1.29–1.10 (m, 2H), 1.06–0.80 (m, 2H). ^{13}C NMR (101 MHz, CDCl_3) δ 142.4, 132.1, 130.7, 130.1, 130.0, 128.2, 70.3, 59.6, 54.1, 48.2, 34.1, 34.1, 32.3, 31.8, 31.0, 29.4, 22.1. LC-MS (ESI+) m/z calcd. for $\text{C}_{17}\text{H}_{23}\text{Cl}_2\text{NO}$ $[(\text{M} + \text{H})]^+$: 328.12; found: 328.05. HPLC t_R : 8.772 min.

***trans*-4-(((1*R*,2*S*)-2-(3,4-Dichlorophenyl)cyclopentyl)amino)cyclohexan-1-ol (33b).** White solid (82.1 mg, 0.25 mmol,

30%). ^1H NMR (400 MHz, CDCl_3) δ 7.36 (d, J = 8.3 Hz, 1H), 7.34 (d, J = 2.1 Hz, 1H), 7.09 (dd, J = 8.3, 2.1 Hz, 1H), 3.51 (tt, J = 10.5, 4.0 Hz, 1H), 3.19 (q, J = 8.1 Hz, 1H), 2.73 (q, J = 8.8 Hz, 1H), 2.40 (tt, J = 10.7, 3.6 Hz, 2H), 2.29 (br s, OH and NH), 2.17–2.07 (m, 2H), 1.98–1.72 (m, 6H), 1.69–1.46 (m, 2H), 1.29–0.90 (m, 4H). ^{13}C NMR (101 MHz, CDCl_3) δ 144.7, 132.5, 130.5, 130.2, 129.4, 126.9, 70.1, 63.6, 54.6, 52.2, 34.1, 34.0, 34.0, 33.2, 31.6, 30.9, 22.9. LC-MS (ESI+) m/z calcd. for $\text{C}_{17}\text{H}_{23}\text{Cl}_2\text{NO}$ $[(\text{M} + \text{H})]^+$: 328.12; found: 328.05. HPLC t_R : 8.968 min.

***cis*-4-(((1*S*,2*S*)-2-(3,4-Dichlorophenyl)cyclopentyl)amino)cyclohexan-1-ol (33c).** Final compound 33c and 33d were obtained from intermediate (*S*)-31 and *cis*-4-aminocyclohexanol hydrochloride following general procedure B at 60 °C. Automatic column chromatography (C18) with 0 to 60% CH_3CN in H_2O + 0.1% TFA as mobile phase on Biotage® Selekt followed by column chromatography on silica gel with 4 to 10% MeOH in DCM as mobile phase. White solid (80.4 mg, 0.25 mmol, 29%). ^1H NMR (400 MHz, CDCl_3) δ 7.36 (d, J = 8.3 Hz, 1H), 7.34 (d, J = 2.1 Hz, 1H), 7.09 (dd, J = 8.3, 2.1 Hz, 1H), 3.79 (tt, J = 5.4, 2.9 Hz, 1H), 3.38 (q, J = 5.7 Hz, 1H), 3.18–3.10 (m, 1H), 2.33 (tt, J = 7.8, 3.5 Hz, 1H), 2.03–1.84 (m, 4H), 1.76–1.19 (m, 12H). ^{13}C NMR (101 MHz, CDCl_3) δ 142.4, 132.1, 130.7, 130.1, 130.0, 128.3, 67.0, 59.2, 52.7, 48.5, 32.3, 31.3, 31.2, 29.3, 28.3, 27.3, 22.2. LC-MS (ESI+) m/z calcd. for $\text{C}_{17}\text{H}_{23}\text{Cl}_2\text{NO}$ $[(\text{M} + \text{H})]^+$: 328.12; found: 328.05. HPLC t_R : 9.023 min.

***cis*-4-(((1*R*,2*S*)-2-(3,4-Dichlorophenyl)cyclopentyl)amino)cyclohexan-1-ol (33d).** Transparent oil (89.0 mg, 0.27 mmol, 33%). ^1H NMR (400 MHz, CDCl_3) δ 7.37–7.33 (m, 2H), 7.10 (dd, J = 8.3, 2.1 Hz, 1H), 3.83–3.70 (m, 1H), 3.19 (q, J = 8.1 Hz, 1H), 2.74 (q, J = 8.6 Hz, 1H), 2.60–2.28 (m, 3H), 2.18–2.05 (m, 2H), 1.89–1.72 (m, 2H), 1.69–1.32 (m, 10H). ^{13}C NMR (101 MHz, CDCl_3) δ 144.7, 132.4, 130.4, 130.0, 129.3, 126.9, 66.3, 63.1, 53.3, 52.2, 33.8, 33.0, 31.2, 31.0, 28.0, 26.9, 22.8. LC-MS (ESI+) m/z calcd. for $\text{C}_{17}\text{H}_{23}\text{Cl}_2\text{NO}$ $[(\text{M} + \text{H})]^+$: 328.12; found: 328.05. HPLC t_R : 9.257 min.

Molecular pharmacology

Reagents and materials. Jump-In™ T-REx™ human embryonic kidney 293 cells (HEK293-JumpIn) cells with doxycycline-inducible expression of human NET (HEK293-JumpIn-NET) were kindly provided by the RESOLUTE consortium (<http://re-solute.eu>). Nisoxetine hydrochloride was purchased from Santa Cruz biotechnology (Dallas, TX, USA).

Cell culture. HEK293-JumpIn-NET cells were grown in Dulbecco's modified Eagles medium (DMEM) supplemented with 10% fetal bovine serum (FBS), penicillin (100 $\mu\text{g mL}^{-1}$) and streptomycin (50 $\mu\text{g mL}^{-1}$) at 37 °C with 5% CO_2 . Cells were subcultured twice weekly at a ratio of 1:15.

NET TRACT assay. To investigate NET inhibition capacity of cycloalkylamine derivatives a 'transport activity through receptor activation' assay (TRACT) was performed utilizing the xCELLigence real-time cell analyzer (RTCA) as reported

previously.^{20,23} The TRACT assay measure NET inhibition indirectly by monitoring the change in cell morphology induced by norepinephrine-mediate activation of α_2 adrenergic receptors that are endogenously present on HEK-cells and co-express NET. Inhibition of NET on these cells will result in increased activation of α_2 adrenergic receptors (*i.e.* enhancement) as NE-uptake by NET is inhibited which is detected as an increased cellular response in the xCELLigence system.

In brief, HEK293-JumpIn-NET cells (60.000 cells per well) with endogenous expression of adrenergic receptors were seeded on 96-well E-plates and grown for 22 h. Cells were pretreated with 1 μ M (screening mode) or increasing concentrations (ranging from 10^{-5} M to 10^{-11} M) of cycloalkylamine derivative or control inhibitor nisoxetine for 1 h. Subsequently, cells were stimulated with 1 μ M norepinephrine (NE) and changes in cellular response were continuously monitored every 15 seconds for 30 minutes. To obtain enhancement or dose-response curves the netAUC over 30 minutes was calculated from the time traces and % enhancement was set at 100% for control inhibitor nisoxetine.

Data analysis. All experimental data were analyzed using GraphPad Prism 10.1.0 (GraphPad Software Inc., San Diego, CA, USA). Data shown represent mean \pm SEM of at least three individual experiments each performed in duplicate. Statistical differences in pIC₅₀ values were analyzed using an ordinary one-way ANOVA with Dunnett's *post hoc* test. Significant differences are displayed as * $p < 0.05$, ** $p < 0.01$ and *** $p < 0.001$.

Molecular docking

The apo structure model of the human NET was retrieved from the EMBL-EBI AlphaFold Protein Structure Database,⁵⁰ the structure was truncated from residue 1 to 55, as this part of the model had low confidence. To properly insert the sodium and chloride atoms in the binding site, the sequence of wildtype NET was retrieved from UniProt and a BLAST search was performed against sequences with an available structure deposited in the PDB.⁵¹ The most similar structure from this search, the *Drosophila melanogaster* dopamine transporter with NET-like mutations,²² was aligned to the AlphaFold model and the coordinates of the ions were kept. After this step, the protein was prepared for molecular docking using Maestro's (v2022-3) protein preparation wizard, including an energy minimization step. Thereafter, a docking grid was generated around the binding site and prepared for docking with GLIDE.⁵² Stereoisomers **32a** and **33b** were generated using LigPrep and consequently docked using GLIDE. The pocket was furthermore analyzed using SiteMap.⁵³ Following docking, the results were filtered and analyzed regarding their predicted docking scores and interactions. Images were generated using PyMOL version 2.5.2.⁵⁴

Data availability

The data supporting this article have been included as part of the ESI.†

Author contributions

Conceptualization: M. A. D., A. P. IJ. and D. v. d. E.; investigation: M. A. D., T. A. M. M., P. M. and W. J.; data curation, formal analysis and validation: M. A. D., T. A. M. M., P. M. and W. J.; funding resources and supervision: G. J. P. v. W., L. H. H., A. P. IJ. and D. v. d. E.; writing – original draft: M. A. D., T. A. M. M. and W. J.; writing – reviewing and editing: M. A. D., T. A. M. M., G. J. P. v. W., L. H. H., A. P. IJ., W. J. and D. v. d. E.

Conflicts of interest

There are no conflicts to declare.

Acknowledgements

We want to thank Rongfang Liu for conducting the fluorescent uptake assay experiments. This project is part of the RESOLUTE project (<https://re-solute.eu>). RESOLUTE has received funding from the Innovative Medicines Initiative 2 Joint Undertaking under grant agreement No. 777372. This Joint Undertaking receives support from the European Union's Horizon 2020 research and innovation programme and EFPIA. This article reflects only the authors' views and neither IMI nor the European Union and EFPIA are responsible for any use that may be made of the information contained therein.

References

- 1 R. V. Parsey, R. S. Hastings, M. A. Oquendo, Y. Huang, N. Simpson, J. Arcement, Y. Huang, R. T. Ogden, R. L. Van Heertum, V. Arango and J. J. Mann, *Am. J. Psychiatry*, 2006, **163**, 52–58.
- 2 A. Mané, J. Gallego, F. Lomeña, J. J. Mateos, E. Fernandez-Egea, G. Horga, A. Cot, J. Pavia, M. Bernardo and E. Parellada, *Psychiatry Res., Neuroimaging*, 2011, **194**, 79–84.
- 3 P. Huot, S. H. Fox and J. M. Brotchie, *J. Parkinson's Dis.*, 2015, **2015**, 1–71.
- 4 J. J. Winrow, C. J. Gotter, A. J. Coleman, P. J. Hargreaves and R. Renger, *Drug Discovery for Psychiatric Disorders*, The Royal Society of Chemistry, 2012.
- 5 J. Prins, B. Olivier and S. M. Korte, *Expert Opin. Invest. Drugs*, 2011, **20**, 1107–1130.
- 6 R. M. A. de Bie, C. E. Clarke, A. J. Espay, S. H. Fox and A. E. Lang, *Lancet Neurol.*, 2020, **19**, 452–461.
- 7 A. S. Kristensen, J. Andersen, T. N. Jørgensen, L. Sørensen, J. Eriksen, C. J. Loland, K. Strømgaard and U. Gether, *Pharmacol. Rev.*, 2011, **63**, 585–640.
- 8 E. Szabadi, *J. Psychopharmacol.*, 2013, **27**, 659–693.
- 9 S. Bröer and U. Gether, *Br. J. Pharmacol.*, 2012, **167**, 256–278.

- 10 V. A. Nazarova, A. V. Sokolov, V. N. Chubarev, V. V. Tarasov and H. B. Schiöth, *Front. Pharmacol.*, 2022, **13**, 1066988.
- 11 L. Sørensen, J. Andersen, M. Thomsen, S. M. R. Hansen, X. Zhao, A. Sandelin, K. Strømgaard and A. S. Kristensen, *J. Biol. Chem.*, 2012, **287**, 43694–43707.
- 12 V. Krishnan and E. J. Nestler, *Nature*, 2008, **455**, 894–902.
- 13 G. I. Papakostas, J. C. Nelson, S. Kasper and H.-J. Möller, *Eur. Neuropsychopharmacol.*, 2008, **18**, 122–127.
- 14 Z. Chen, J. Yang and P. Skolnick, in *Transporters as Targets for Drugs*, ed. S. Napier and M. Bingham, Springer Berlin Heidelberg, Berlin, Heidelberg, 2008, pp. 131–154.
- 15 R. Costa, N. G. Oliveira and R. J. Dinis-Oliveira, *Drug Metab. Rev.*, 2019, **51**, 293–313.
- 16 A. Cipriani, T. A. Furukawa, G. Salanti, A. Chaimani, L. Z. Atkinson, Y. Ogawa, S. Leucht, H. G. Ruhe, E. H. Turner, J. P. T. Higgins, M. Egger, N. Takeshima, Y. Hayasaka, H. Imai, K. Shinohara, A. Tajika, J. P. A. Ioannidis and J. R. Geddes, *Lancet*, 2018, **391**, 1357–1366.
- 17 S. M. Stahl, M. M. Grady, C. Moret and M. Briley, *CNS Spectr.*, 2005, **10**, 732–747.
- 18 A. J. Rush, M. H. Trivedi, S. R. Wisniewski, J. W. Stewart, A. A. Nierenberg, M. E. Thase, L. Ritz, M. M. Biggs, D. Warden, J. F. Luther, K. Shores-Wilson, G. Niederehe and M. Fava, *N. Engl. J. Med.*, 2006, **354**, 1231–1242.
- 19 A. E. L. L. Walsh, N. T. M. M. Huneke, R. Brown, M. Browning, P. Cowen and C. J. Harmer, *Front. Psychiatry*, 2018, **9**, 482.
- 20 B. J. Bongers, H. J. Sijben, P. B. R. R. Hartog, A. Tarnovskiy, A. P. IJzerman, L. H. Heitman and G. J. P. van Westen, *J. Chem. Inf. Model.*, 2023, **63**, 1745–1755.
- 21 W. Xue, T. Fu, G. Zheng, G. Tu, Y. Zhang, F. Yang, L. Tao, L. Yao and F. Zhu, *Curr. Med. Chem.*, 2020, **27**, 3830–3876.
- 22 S. Pidathala, A. K. Mallela, D. Joseph and A. Penmatsa, *Nat. Commun.*, 2021, **12**, 2199.
- 23 H. J. Sijben, W. M. van Oostveen, P. B. R. Hartog, L. Stucchi, A. Rossignoli, G. Maresca, L. Scarabottolo, A. P. IJzerman and L. H. Heitman, *Sci. Rep.*, 2021, **11**, 12290.
- 24 L. Shao, F. Wang, S. C. Malcolm, M. C. Hewitt, J. Ma, S. Ribe, M. A. Varney, U. Campbell, S. R. Engel, L. W. Hardy, P. Koch, R. Schreiber and K. L. Spear, WO2008151156A1, Sepracor Inc., 2008.
- 25 L. Shao, M. C. Hewitt, F. Wang, S. C. Malcolm, J. Ma, J. E. Campbell, U. C. Campbell, S. R. Engel, N. A. Spicer, L. W. Hardy, R. Schreiber, K. L. Spear and M. A. Varney, *Bioorg. Med. Chem. Lett.*, 2011, **21**, 1438–1441.
- 26 L. Shao, M. C. Hewitt, F. Wang, S. C. Malcolm, J. Ma, J. E. Campbell, U. C. Campbell, S. R. Engel, N. A. Spicer, L. W. Hardy, R. Schreiber, K. L. Spear and M. A. Varney, *Bioorg. Med. Chem. Lett.*, 2011, **21**, 1434–1437.
- 27 D. T. Wong, P. G. Threlkeld, K. L. Best and F. P. Bymaster, *J. Pharmacol. Exp. Ther.*, 1982, **222**, 61–65.
- 28 L. Shao, M. C. Hewitt, S. C. Malcolm, F. Wang, J. Ma, U. C. Campbell, N. A. Spicer, S. R. Engel, L. W. Hardy, Z. Jiang, R. Schreiber, K. L. Spear and M. A. Varney, *J. Med. Chem.*, 2011, **54**, 5283–5295.
- 29 Y. Ishichi, E. Kimura, E. Honda, M. Yoshikawa, T. Nakahata, Y. Terao, A. Suzuki, T. Kawai, Y. Arakawa, H. Ohta, N. Kanzaki, H. Nakagawa and J. Terauchi, *Bioorg. Med. Chem.*, 2013, **21**, 4600–4613.
- 30 F. Micheli, P. Cavanni, R. Arban, R. Benedetti, B. Bertani, M. Bettati, L. Bettelini, G. Bonanomi, S. Braggio, A. Checchia, S. Davalli, R. Di Fabio, E. Fazzolari, S. Fontana, C. Marchioro, D. Minick, M. Negri, B. Oliosi, K. D. Read, I. Sartori, G. Tedesco, L. Tarsi, S. Terreni, F. Visentini, A. Zocchi and L. Zonzini, *J. Med. Chem.*, 2010, **53**, 2534–2551.
- 31 M. A. M. M. Subbaiah, *J. Med. Chem.*, 2018, **61**, 2133–2165.
- 32 P. Wang, X. Zhang, T. Fu, S. Li, B. Li, W. Xue, X. Yao, Y. Chen and F. Zhu, *ACS Chem. Neurosci.*, 2017, **8**, 1416–1428.
- 33 V. Bisagno, B. González and F. J. Urbano, *Pharmacol. Res.*, 2016, **109**, 108–118.
- 34 L. Shao, F. Wang, S. C. Malcolm, J. Ma, M. C. Hewitt, U. C. Campbell, L. R. Bush, N. A. Spicer, S. R. Engel, L. D. Saraswat, L. W. Hardy, P. Koch, R. Schreiber, K. L. Spear and M. A. Varney, *Bioorg. Med. Chem.*, 2011, **19**, 663–676.
- 35 G. B. Baker and T. I. Prior, *Ann. Med.*, 2002, **34**, 537–543.
- 36 V. Y. Yevtushenko, A. I. Belous, Y. G. Yevtushenko, S. E. Gusinin, O. J. Buzik and T. V. Agibalova, *Clin. Ther.*, 2007, **29**, 2319–2332.
- 37 R. U. McVicker and N. M. O'Boyle, *J. Med. Chem.*, 2024, **67**, 2305–2320.
- 38 N. D. Danchev, V. V. Rozhanets, L. A. Zhmurenko, O. M. Glozman and V. A. Zagorevskii, *Bull. Exp. Biol. Med.*, 1984, **97**, 576–578.
- 39 N. Benson, N. Snelder, B. Ploeger, C. Napier, H. Sale, N. J. M. Birdsall, R. P. Butt and P. H. van der Graaf, *Br. J. Pharmacol.*, 2010, **160**, 389–398.
- 40 C. Orrenius, F. Hbffer, D. Rotticci, N. Öhrner, T. Norin and K. Hult, *Biocatal. Biotransform.*, 1998, **16**, 1–15.
- 41 J. A. Aikins, E. C. R. Smith, T. A. Shepherd and D. M. Zimmerman, WO2001042203A1, Eli Lilly and Company, 2001.
- 42 P. Kalaba, K. Pacher, P. J. Neill, V. Dragacevic, M. Zehl, J. Wackerlig, M. Kirchhofer, S. B. Sartori, H. Gstach, S. Kouhnavardi, A. Fabisikova, M. Pillwein, F. Monje-Quiroga, K. Ebner, A. Prado-Roller, N. Singewald, E. Urban, T. Langer, C. Pifl, J. Lubec, J. J. Leban and G. Lubec, *Biomolecules*, 2023, **13**, 1415.
- 43 H. Zhang, Y.-L. Yin, A. Dai, T. Zhang, C. Zhang, C. Wu, W. Hu, X. He, B. Pan, S. Jin, Q. Yuan, M.-W. Wang, D. Yang, H. E. Xu and Y. Jiang, *Nature*, 2024, **630**, 247–254.
- 44 G. Tu, T. Fu, F. Yang, J. Yang, Z. Zhang, X. Yao, W. Xue and F. Zhu, *ACS Chem. Neurosci.*, 2021, **12**, 2013–2026.
- 45 V. Navratna and E. Gouaux, *Curr. Opin. Struct. Biol.*, 2019, **54**, 161–170.
- 46 F. A. Paczkowski, I. A. Sharpe, S. Dutertre and R. J. Lewis, *J. Biol. Chem.*, 2007, **282**, 17837–17844.
- 47 C.-I. A. Wang, N. H. Shaikh, S. Ramu and R. J. Lewis, *Mol. Pharmacol.*, 2012, **82**, 898–909.
- 48 S. K. Singh, A. Yamashita and E. Gouaux, *Nature*, 2007, **448**, 952–956.

- 49 A. V. Pedersen, T. F. Andreassen and C. J. Loland, *J. Biol. Chem.*, 2014, **289**, 35003–35014.
- 50 M. Varadi, S. Anyango, M. Deshpande, S. Nair, C. Natassia, G. Yordanova, D. Yuan, O. Stroe, G. Wood, A. Laydon, A. Židek, T. Green, K. Tunyasuvunakool, S. Petersen, J. Jumper, E. Clancy, R. Green, A. Vora, M. Lutfi, M. Figurnov, A. Cowie, N. Hobbs, P. Kohli, G. Kleywegt, E. Birney, D. Hassabis and S. Velankar, *Nucleic Acids Res.*, 2022, **50**, D439–D444.
- 51 H. M. Berman, *Nucleic Acids Res.*, 2000, **28**, 235–242.
- 52 R. A. Friesner, J. L. Banks, R. B. Murphy, T. A. Halgren, J. J. Klicic, D. T. Mainz, M. P. Repasky, E. H. Knoll, M. Shelley, J. K. Perry, D. E. Shaw, P. Francis and P. S. Shenkin, *J. Med. Chem.*, 2004, **47**, 1739–1749.
- 53 T. A. Halgren, *J. Chem. Inf. Model.*, 2009, **49**, 377–389.
- 54 W. L. DeLano, *The PyMOL Molecular Graphics System, Version 2.5.2*, Schrödinger, LLC, New York, NY, 2021.